Spectrochimica Acta Part A: Molecular and Biomolecular Spectroscopy 249 (2021) 119308

Contents lists available at ScienceDirect

Spectrochimica Acta Part A: Molecular and Biomolecular Spectroscopy

journal homepage: www.elsevier.com/locate/saa

Electrospun poly (vinyl alcohol) nanofibers incorporating caffeic acid/cyclodextrins through the supramolecular assembly for antibacterial activity

Vimalasruthi Narayanan [a], Manawwer Alam [b], Naushad Ahmad [b], Suganya Bharathi Balakrishnan [a], Vigneshkumar Ganesan [a], Esakkimuthu Shanmugasundaram [a], Brindha Rajagopal [a], Stalin Thambusamy [a,*]

[a] Department of Industrial Chemistry, Alagappa University, Karaikudi 630002, Tamil Nadu, India
[b] Department of Chemistry, College of Science, King Saud University, Riyadh 11451, Saudi Arabia

HIGHLIGHTS

- CA/CDs embedded electrospun nanofibers were successfully fabricated via electrospinning technique.
- Complex formation was characterized by FT-IR, UV, and Raman-Spectroscopy.
- Enhanced solubility of CA from CA/CDs was confirmed by Phase-Solubility test.
- The dissolution diagram exhibits the dissolution of CA from PVA/CA/CDs more efficient than PVA/CA electrospun nanofibers.

GRAPHICAL ABSTRACT

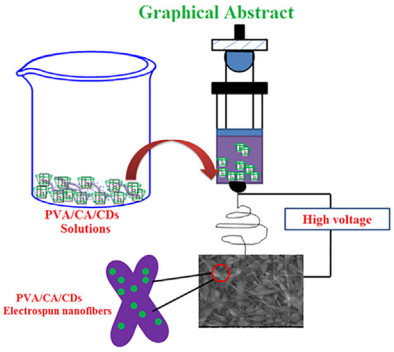

ARTICLE INFO

Article history:
Received 7 September 2020
Received in revised form 24 November 2020
Accepted 1 December 2020
Available online 15 December 2020

Keywords:
Nanofibers
Cyclodextrins
Inclusion complex
Antibacterial activity
Solubility

ABSTRACT

Here, we prepared the solid inclusion complexes between Caffeic acid (CA) and Cyclodextrins (β- and γ-CDs) (CA/CDs) that were effectively embedded into Poly (vinyl alcohol) (PVA) electrospun nanofibers via electrospinning technique to enhanced solubility and antibacterial activity. In tested Cyclodextrins are β- and γ-CDs with CA in the ratio of 1:1 resulting in the formation of CA/CDs by co-precipitation method. The physical properties of CA/CDs were examined by FT-IR, UV, and Raman Spectroscopy. The phase solubility test showed a much higher solubility of CA due to inclusion complexes (ICs). Furthermore, CA/β-CD and CA/γ-CD perfected achieved 0.70:1 and 0.80:1 the molar ratio of ICs, confirmed by NMR studies. The fiber size distribution, average diameter, and morphology features were evaluated by SEM analysis. The dissolution profile of PVA/CA and PVA/CA/CDs were tested within 150 min, resulting in CA dissolved in PVA/CA/CDs slightly higher than PVA/CA nanofibers due to enhanced solubility of ICs. Moreover, PVA/CA/CDs exhibit high antibacterial activity against gram-positive bacteria of *E-Coli* and gram-negative bacteria of *S. aureus*. Finally, these results suggest that PVA/CA/CDs may be promising materials for active food packaging applications.

1. Introduction

The non-biodegradable and non-renewable polymeric composites are more attractive materials due to their unique properties

* Corresponding author.
E-mail address: stalin.t@alagappauniversity.ac.in (S. Thambusamy).

https://doi.org/10.1016/j.saa.2020.119308
1386-1425/

such as low cost, light in weight with a significant degree of strength, corrosion resistance, and act as a thermal and electrical insulator [1,2]. There are various methods used to produce the nanofibers from polymers phase separation [3], template synthesis [4], drawing [5], chemical vapor deposition [6], sol–gel method [7], self-assembly [8], and typically is electrospinning. It has received electrospun nanofibers by electrical force to enhance the chemical and physical properties of polymers [9–11]. First, Introduced in Formhals fiber manufacture in the year 1944, and they moved in industrial applications [12]. Followed various nanostructures developed for different fields of nanofibers that are more favorable compared to others. They have significant physicochemical properties such as high surface to volume ratio, lightweight with small diameter, controllable pores structure, and flexibility of surface modifications. The synthetic polymer is having a large molecular weight, a high thermal property, and mechanical stability. So, these are preferable to fabricating the electrospun nanofibers compared to natural biopolymers [13–18]. Electrospinning of nanofibers with cyclodextrins (CDs) or Cyclodextrins inclusion complexes(CDs/ICs) nanofibers was most attractive materials for material science due to cost-effective technique for producing the continues functional nanofibers from biodegradable polymers like Polyvinyl alcohol (PVA)[19], Polyethylene glycol(PEG)[20], Polyvinylpyrrolidone (PVP)[21], Polylactic acid (PLA)[22] and Polylactic-co-glycolic acid (PLGA)[23] and Polycaprolactone (PCL)[24]. CDs are polymeric cyclic oligosaccharides is the ability to forming the ICs with a variety of antimicrobial molecules to reduce the volatility. And the control to release antimicrobial compounds enhance the thermal stability, solubility, and bioavailability [25–29]. The most common CDs are α-, β-, and γ-CD containing 6, 7, and 8 glucopyranose units in the cone-shaped structure. These can be forming the complexation [30–33] depending upon their size and shape fit between the host of CDs and guest of antibacterial molecules [34–36]. It has shown unique properties are enhance like solubility binding strength [37,38] is interestedly and appealing in the application of different fields like textiles, cosmetics, tissue engineering, pharmaceutical, drug delivery, and food chemistry [39–43]. Researchers are fabricated in Menthol [44], Eugunol [45], Vanillin [46,47], Essential oil [48], gallic acid [49], Triclon [50], etc., Encapsulated CDs/ICs with supporting polymers like PVA, PMMA, and PVP electrospun nanofibers electrospinning technique. It is applicable in food packaging and flavoring agent in the food industry [51–54].

Caffeic acid (CA) is a hydrophobic polyphone which appeared in the phenolic compound, extracting in aromatic leaves used in the cosmetic and food industry. Due to highly anti-oxidant, antibacterial, anti-allergic, and anti-inflammatory activity. Unfortunately, it has unfavorable properties such as volatility, low solubility, and less thermal stability [55,56]; overcome this problem by introducing the host–guest complexation due to CA perfectly including with CDs to form ICs [57]. For more than fifteen years, the corresponding author research group has been involving in studying the complexation properties [58–63]. It is stimulating us to carry out a study on Caffeic acid inclusion complexes to examine the possibility of complex formation with β-CD and γ-CD. Particularly in solid-state to improve its dissolution profile and control the releasing capability of antimicrobial agents and enhance the antibacterial activity. For a recent we have observed the fabrication of CDs/ICs into polymeric electrospun nanofibers not only specific properties of CDs/ICs and also exhibits the high surface area and nonporous structure. Polyvinyl alcohol (PVA) is a biocompatible and biodegradable non-toxic synthetic polymer. Mainly it's highly water-soluble, broadly used in food chemistry and the field of the biomedical industry [64,65]. In the present study, first, we prepared a 1:1 M ratio of modified β-, and γ-CDs with CA to forming CA/CDs. It is confirming by FT-IR, UV, and Raman studies. CA/γ-CD achieved higher binding efficiency compared to CA/β-CD, confirmed by NMR studies. Besides, we calculate the binding properties and solubility of CA/CDs with the phase solubility diagram. These CA/β-CD and CA/γ-CD encapsulated PVA electrospun nanofiber by electrospinning technique under optimal conditions. The prepared PVA, PVA/CA nanofibers as a comparison. The average fiber distribution (AFD) and Average roughness (AR), and surface morphology were by SEM analysis. In the dissolution profile on CA from PVA/CA and PVA/CA/CDs nanofibers studied in UV-Spectroscopy at 283 nm. The antibacterial studies were investigating against gram-positive bacteria (*s.aureus*) and gram-negative bacteria (*E.coli*). And have enhanced the antibacterial activity of the electrospun nanofibers (PVA /CA/CDs). Finally, our results suggest that CA/CDs encapsulating Polymeric nanofibers were may be suitable materials for food packaging due to enhanced solubility of CA and antibacterial activity.

2. Experimental details

2.1. Materials

Caffeic acid (98%, TCI Co., LTD.), Polyvinylalcohol (PVA, MW 60,000–1,25,000 g mol^{-1}, Viscosity 9.00–21.00 cp HIMEDIA), Deuterated dimethyl sulfoxide (DMSO d_6, Merk for NMR Spectroscopy) *beta*-cyclodextrin and *gamma*-cyclodextrin (β-CD and γ-CD, SRL Co., LTD.) was purchased and used as without any further purifications. The water was from Miliporoe Milli-Q ultrapure water system.

2.2. Preparation of solid inclusion complex (CD/CA)

The chemical structure of CA, β-CD, and γ-CD is showing in Fig. 1a. ICs prepared by mixing the 1:1 M ratio of CA and each CD according to the Co-Precipitation method, schematically representing as Fig. 1b. In brief, the mixture of CDs (1 g /0.003 mol) and CA (0.12 g/0.003 mol) was dissolved in 20 mL water, stirring for 24 h dark at RT. Further, the precipitate was collected by filtration using filter paper and washed several times. With purified water to remove the un-reacted CA and CDs. Which are drying in a vacuum, finally white powder product (both β-CD and γ-CD/CA) is obtained.

2.3. Preparation of electrospinning solution

PVA/CA/CDs nanofibers produced using the electrospinning method. This experimental schematic representation is showing in Fig. 1c. To prepare the PVA/CA/CDs solutions and PVA (16% w/v) was dissolved in water. 10% CA/CDs and 5% CA (w/w, concerning polymer) were dissolving in water at RT. First, the solution (PVA) has prepared separately. 1.6 g of PVA pellets were dissolved in water for 4 h at 75 °C are cooled at RT. These CA/β-CD and CA/γ-CD solutions were adding to the polymeric (PVA) solution. Furthermore, they were stirring for 2 h at RT; for comparison. The without CD solutions of pristine PVA and PVA/CA were preparing as the same method. These polymeric solutions have been placing into the electrospinning setup.

2.4. Electrospinning

Each polymeric solution has placed into a 10 mL syringe having a metallic needle with 0.8 mm inner diameter. The syringe has positioned vertically on the syringe pump. Electrospinning parameters were as follows, a flow rate of the polymer solution was 1 mL/h, the applied voltage 20 kV, and the needle to collector distance was 10 cm. The fibers have been collecting by the grounded stationary cylindrical collector and are covering with aluminum foil. Electrospinning whole setup was performing at 23 °C and

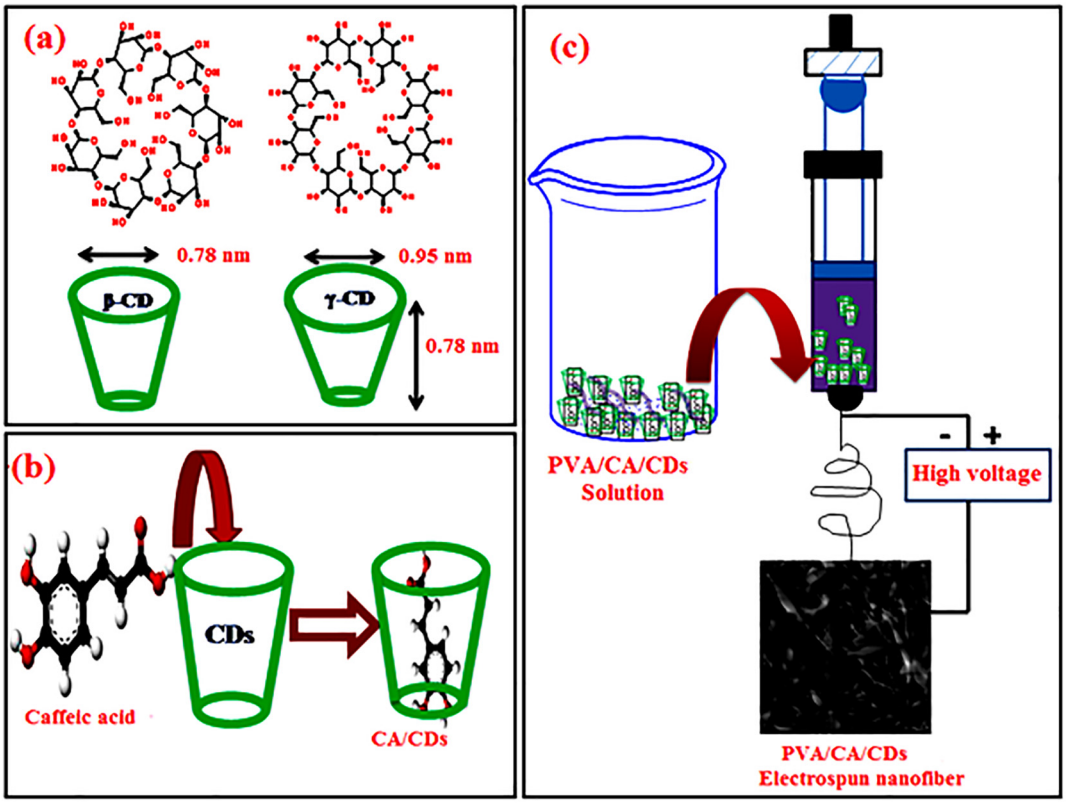

Fig. 1. (a) Chemical structure and approximate dimension of β-CD and γ-CD (b) Formation of CA/CDs and (c) Electrospinning of nanofibers from PVA/CA/CDs solution.

18% relative humidity in an enclosed box. Finally, preparing nanofibers have dried at room temperature to remove the residual solvent and stored at 4 °C for further characterization.

2.5. Materials characterization

The electrospun nanofibers have been synthesizing using in the laboratory by using electrospinning. The equipment is ESPIN-NANO from the physics Instrument Company, Chennai. Phase solubility measurement is have carried out by the method of Higuchi and corners [66]. An excess amount of CA was adding to the aqueous solution of β-CD, and γ-CD (range 5 to 50 mM) solution was stirred in 12 h at RT that the solution has filtered. The un-dissolved CA has been removing. The concentration of CA has calculated spectrometrically at 283 nm. Moreover, the stability constant has been determining by the following equation.,

$$K_s = \text{Slope}/S_0(1 - \text{Slope}) \quad (1)$$

where S_0, the solubility of CA without CDs finally the phase solubility graph was plotting in Concentration of CA versus concentration CDs.

CD/CA characterizations have by FT-IR (Fourier transform infrared spectroscopy), UV (Ultra Violet spectroscopy), ^{1}H NMR (proton nuclear magnetic resonance spectroscopy), and Raman-Spectroscopy. The pristine CA is also characterizing for comparison. The molar ratio between CA and CD is have examined by the ^{1}H NMR (^{1}HNMR, Bruker D PX-400) system. It was dissolving in d^6-DMSO at the 20 g/L concentration.

The spectra have been recording at 400 MHz and 16 total scans. The Mestrenova software has been using to identify the integration of chemical shift value (ppm) and calculating the molar ratio of CA and CD. The FT-IR spectroscopy is using to analyze the interaction between the guest–host ICs and identify the functional group of CA and CDs; the spectra were recorded from 450 to 4000 cm^{-1}, at a resolution of 4 cm^{-1}, by taking 64 scans for each sample (FT/IR-4600 type in KBr mode). Electronic transitions of inclusion complex are determining by Ultraviolet (UV) spectrometry (Jasco V530 UV Visible spectrophotometer). The spectra have recorded the range of 200–800 cm^{-1}. PVA, PVA/CA/β-CD, and PVA/CA/γ-CD are characterizing by using Scanning Electrons Microscopy (SEM) (VEGA 3 TESCAN) with a working distance of 8 mm. The dissolution profile of PVA/CA, PVA/CA/β-CD, and PVA/CA/ γ-CD nanofibers has been carrying out by using UV spectroscopy (Shimadzu UV-2401 Spectrometer). Equivalent (10 mg) amount of each nanofiber dissolving in 20 mL Mili Q water and the solution was stirring at RT, 500 rpm for three hours. At different time intervals

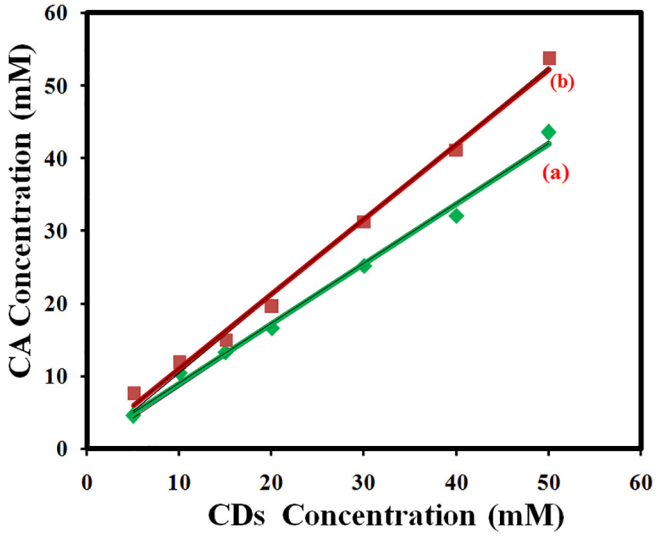

Fig. 2. Phase solubility diagram of (a) CA/β-CD and (b) CA/γ-CD.

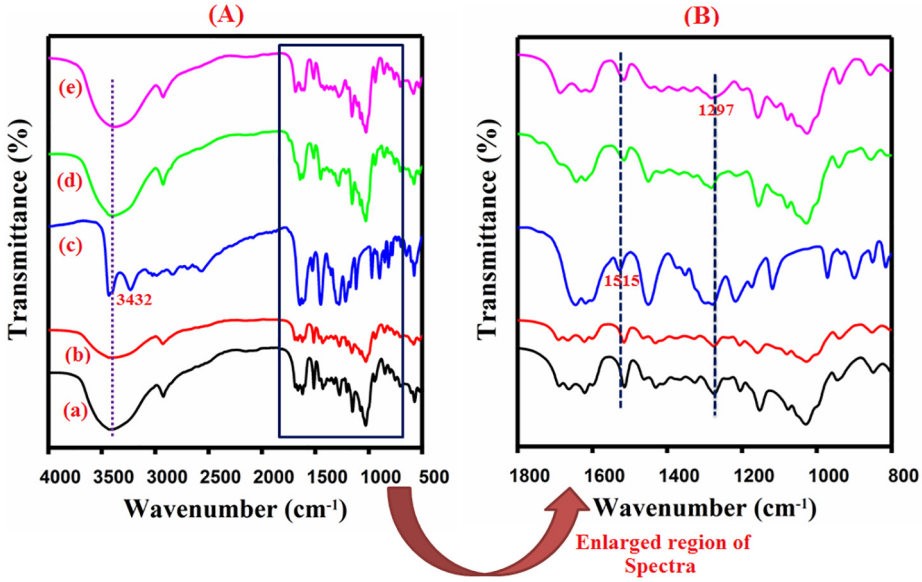

Fig. 3. (A). FT-IR spectra of (a) β-CD, (b) γ-CD, (c) CA, (d) CA/β-CD and (e) CA/γ-CD, (B). Enlarged region of FT-IR spectra between 1800 and 800 cm^{-1} of (a) β-CD, (b) γ-CD, (c) CA, (d) CA/β-CD and (e) CA/γ-CD.

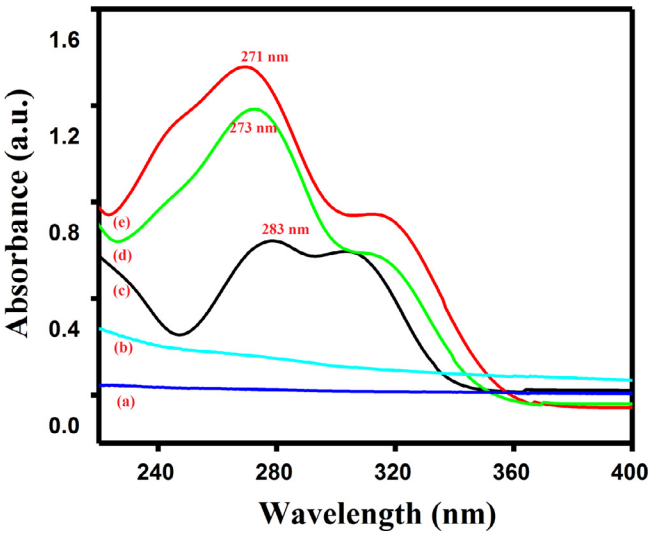

Fig. 4. UV Spectra of (a) β-CD, (b) γ-CD (c) CA, (d) CA/β-CD and (e) CA/γ-CD.

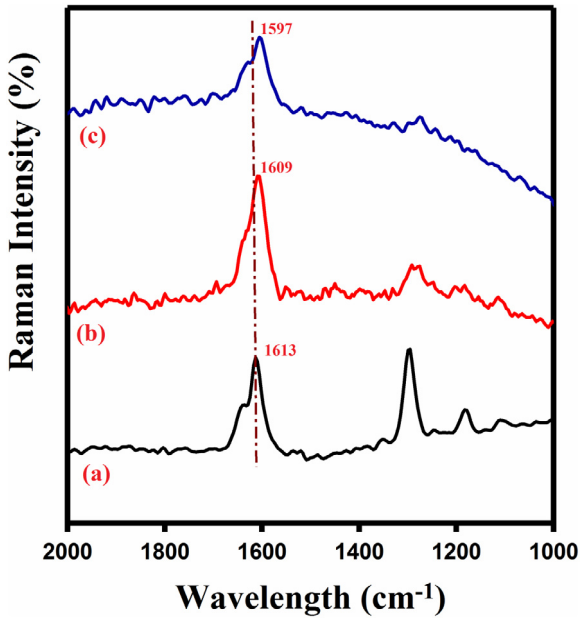

Fig. 5. Raman-Spectra of (a) CA, (b) CA/β-CD and (c) CA/γ-CD.

(15,30,45,90,120,150 and 180 min) of 3 mL of the solution has withdrawn at the same volume of fresh water has replaced the solution. The absorbance of the collected solution has evaluated at 283 nm. The bacterial activity of fabricated electrospun nanofibers of PVA/CA/β-CD and PVA/CA/γ-CD have been investigating. It is against the Gram-positive bacteria, *S. aureus* (ATCC-25923). And Gram-negative bacteria, *E. coli* (ATCC-23828) have seeding on the surface of Mueller-Histon agar. This test is doing in-vitro using a disk agar diffusion method. The bacteria were grown overnight and incubated at 37 °C, and then serially diluted 1 X 108 colony-forming units (CFU/ml). First, the nanofibers were cutting into small pieces. It is placing on the top of the solidified medium. After 24 h of incubation, the inhibition zone and diameter has recorded. The experiment is carrying out with triplicate determination.

3. Result and discussion

3.1. Phase solubility study

The CA/β-CD and CA/γ-CD phase solubility diagram is representing in Fig. 2. The figure displayed by the AL type, which means the CA concentration increased linearly increase the CDs concentration, confirming enhancing solubility of CA due to ICs [67]. The linear trend expresses the 1:1 (guest: host) molecular complex formation. The binding strength between the CA and CDs is have calculated by equation (1). The stability constants are calculating as 738 M^{-1} and 1217 M^{-1} for CA/β-CD and CA/γ-CD. This result suggests that the stable complex formation between both CDs.

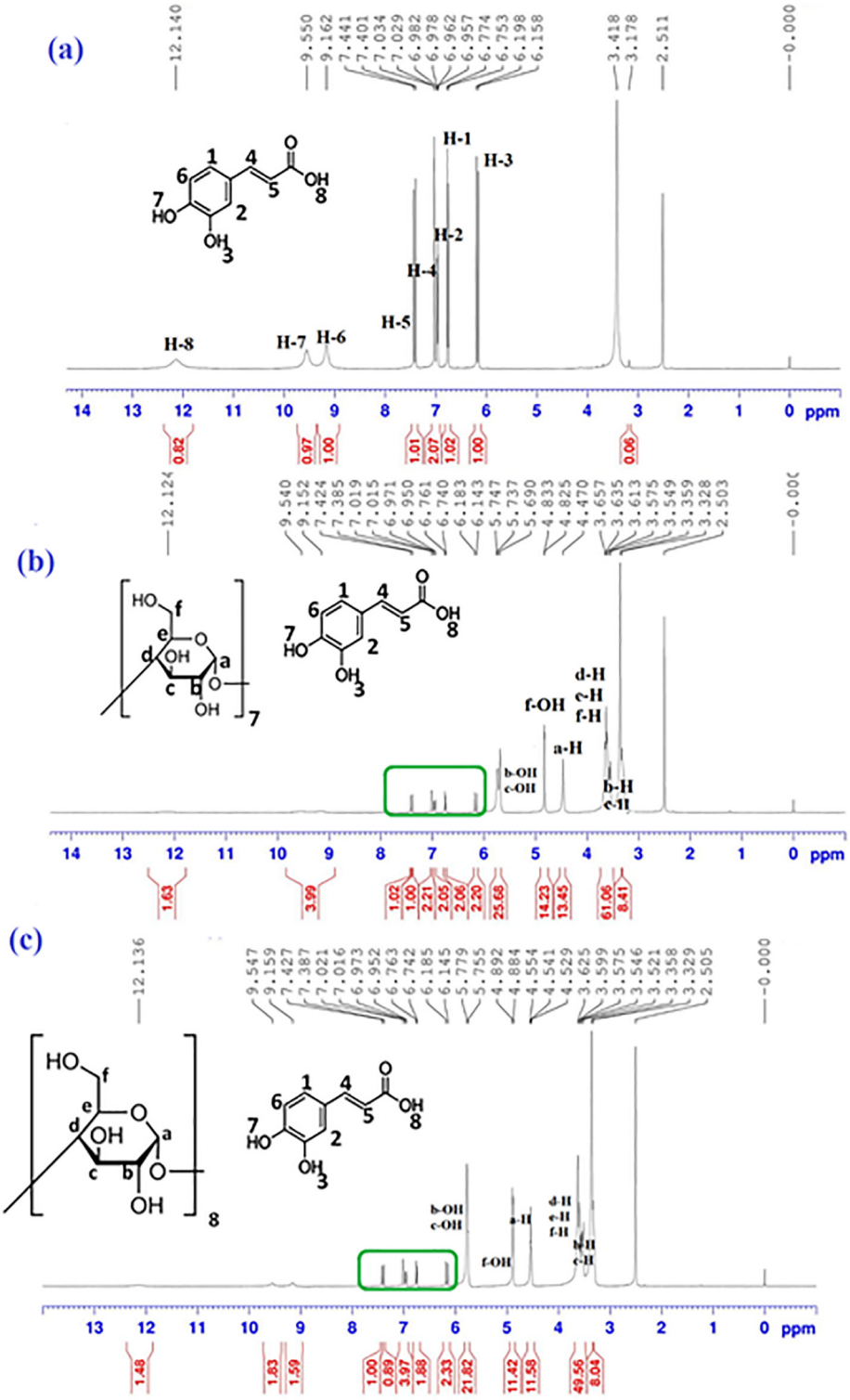

Fig. 6. ^{1}H NMR Spectra of (a)CA (b) CA/β-CD and (c) CA/γ-CD.

3.2. FT-IR analysis

The Chemical interaction between host and guest is studying by using FT-IR spectroscopy. Fig. 3 exhibits the FT-IR spectra of the prepared inclusion complex and CA for comparison. The FT-IR spectra of CA consisted of a series of sharp two peaks 1664 cm^{-1} indicate stretching vibration of C—O groups. The 3432 and 3232 cm^{-1} attributed the hydroxyl group and aromatic conjugated carbonyl group. The phenyl nucleus peak is an exhibit at 1297 cm^{-1} [68]. The γ-CD peaks observed at 2968 and 1276 cm^{-1} exhibit methyl C-H stretching and C-O-C asymmetric stretching vibrations, whereas β-CD occurs in 2925 and 1272 cm^{-1}[69]. In the case of CA/β-CD and CA/γ-CD and CA were observed, confirming the presence of CA in the complex. The hydroxyl band located at 1686 cm^{-1} had been shifted and diminished in the spectrum of CA/β-CD and CA/γ-CD. Compared to the CA and ICs stretching shift 3432(CA) to 3376 (CA/γ-CD) and 3400 cm^{-1} (CA/β-CD). The phenyl nucleus band of CA at

Table 1
^{1}H NMR chemical shifts of protons of CA_{free} and $CA_{complexed}$ with β-CD in DMSO d_6 solvent.

H assignment	The Chemical shift of CA_{free} (ppm)	The Chemical shift of $CA_{complexed}$ with β-CD	Difference between ($CA_{complexed}$ with β-CD - CA_{free} (ppm))
H-1	12.140(s)	12.124	0.016
H-2	7.441(d)	7.424	0.017
H-3	7.034(d)	7.019	0.018
H-4	6.982(d)	6.971	0.011
H-5	6.962(d)	6.95	0.012
H-6	9.550(s)	9.54	0.01
H-7	9.162(s)	9.152	0.01
H-8	6.774(d)	6.762	0.012

Table 2
^{1}H NMR chemical shifts of protons of CA_{free} and $CA_{complexed}$ with γ-CD in DMSO d_6 solvent.

H assignment	The Chemical shift of CA_{free} (ppm)	$CA_{complexed}$ with γ-CD	Difference between ($CA_{complexed}$ with γ-CD- CA_{free} (ppm))
H-1	12.140(s)	2.136	0.004
H-2	7.441(d)	7.427	0.014
H-3	7.034(d)	7.021	0.013
H-4	6.982(d)	6.973	0.009
H-5	6.962(d)	6.954	0.012
H-6	9.550(s)	9.547	0.003
H-7	9.162(s)	9.159	0.003
H-8	6.774(d)	6.753	0.01

1297 cm^{-1} was observing more intensely and sharply in the case of CA peaks are also observed in the complex. But whereas changed to slightly broadly; moreover, the sharpest absorption peaks are at 1515 cm^{-1} indicates that C═C stretching vibration of an aromatic moiety which peak clearly shown in the spectrum of CA/CDs. Finally, our FT-IR result suggests that CA is deeply embedded into the CD cavity hydrophobically.

3.3. UV analysis

Fig. 4 shows the absorption spectra of CA in the absence and presence of β-CD and γ-CD. Before that, it has dissolved in water. The electronic absorption peak of CA is observing at 283 nm (π-π^* transition phenolic group, hypochromic). And 315 nm (π- π^* transition of the double bond, hyperchromic) [70]. Meanwhile, the absence of the β-CD and γ-CD absorption peaks are observing. Moreover, the intensity peak of CA increased to CA/β-CD and CA/γ-CD. Simultaneously, the absorption wavelength of 284 nm appeared at blue-shifted to 273 (CA/β-CD) nm and 271 nm (CA/γ-CD).

These results suggested that CA hydrophobically interacts with the β-CD and γ-CD cavity.

3.4. Raman analysis

The interaction between CA and CDs is investigating by Raman Spectroscopy. Fig. 5 is attributing to the Raman spectrum of prepared ICs. CA molecules have an aromatic ring so. It's favored to interact with the CDs cavity, furthermore characteristic vibrations and group frequencies in spectral regions free from CDs bands, which properties are useful to probing the guest molecule by complexation. The intensity of the 1613 cm^{-1} peak is attributing to the aromatic C═C vibration spectrum was for studying its inclusion complexation with CD derivatives. The CA/β-CD and CA/γ-CD peak is observing at 1613 cm^{-1}. It shifted to 1609 cm^{-1} and 1597 cm^{-1} the intensity of the spectra is also reducing due to C═C stretching was sensitive to host–guest interaction as a formation of inclusion complex, which is a consequence and localization of single and double bonds [70]. In the C-O stretching (1299 cm^{-1}) is has slightly shifted to 1291 cm^{-1} and 1271 cm^{-1} (CA/β-CD and CA/γ-CD). It indicates that the aromatic ring liked to an inter-link chain of CDs. Finally, these results suggesting that the aromatic ring interacting with the CDs cavity.

3.5. NMR-analysis

The ^{1}H NMR spectra of CA/β-CD, CA/γ-CD, and pure CA are have characterized for comparison spectra are showing in Fig. 6. ICs affected the physical and chemical environment of the host–guest hydrogen molecule explains only the internal surface of hydrogen but not the external hydrogen surface [71]. First, the samples dissolved in a ^{d}6-DMSO solvent for NMR measurement. Tables 1 & 2 summarizes the chemical shift of CA, CA/β-CD, and CA/γ-CD. CA is a highly hydrophobic, CA with β-CD & γ-CD ^{1}H NMR spectra show that induced the upfield changed all protons of CA. CA consists of the five hydrogens are H-2, H-3, H-3, H-4, and H-5, to obtained high delta values of CA/β-CD and CA/γ-CD of H-2 ($\Delta\delta$ = 0.017 & 0.014), H-3 ($\Delta\delta$ = 0.018 & 0.013) and H-5 ($\Delta\delta$ = 0.012 & 0.012) indicates that adjacent —C═C— groups. Furthermore, the molar ratio of CA/β-CD and CA/γ-CD is have calculated as 0.70:1 and 0.80:1 by taking integration peaks ratios of the characteristic chemical shift of CA (6.18 ppm), β-CD (4.37 ppm), and γ-CD (4.47 ppm) means the un-complexed CA was present in ICs. Finally, this result revealed that the CA molecule was deeply including inside the hydrophobic cavity of β-CD & γ-CD and CA/γ-CD complexation efficiency was slightly higher than CA/β-CD.

3.6. Morphology analysis

The morphology of the prepared nanofibers was examined by SEM imaging, which employed the surface morphology of prepared nanofibers in Fig. 7. In uniforms (PVA) and bead-free morphology were obtaining. In the case of PVA/CA beads was obtained, whereas PVA/CA/β-CD and PVA/CA/γ-CD nanofibers showed not uniform morphology because crystalline aggregates of CA/β-CD and CA/γ-CD were present and distributed to the PVA nanofibers. Additionally, the Average Fiber Diameter (AFD) and Average Roughness (AR) of prepared nanofibers are have calculated by using image processing software (ImageJ software) [72]. In the AFD results of PVA, PVA/CA, PVA/CA/β-CD, and PVA/CA/γ-CD found to be AFD 141 ± 10, 114 ± 19, 127 ± 20, and 131 ± 18 nm. Fig. 8 exhibits the AR of the preparing nanofibers are have found in 360 ± 21, 282 ± 40, 320 ± 32, and 370 ± 21 nm. In the case of PVA/CA/β-CD and PVA/CA/γ-CD were higher AR, it's had a crystal with nanofibers surface morphology. The higher AFD were obtained in PVA/CA/β-CD and PVA/CA/γ-CD nanofibers when compared to PVA/CA nanofiber, which is possible to an interaction between the CA/CDs crystals and PVA polymer chain. However, the fibers are have obtained with CA/β-CD, and CA/γ-CD crystalline on their surface indicates the perfectly CA/CDs loaded within the PVA nanofibers [73].

3.7. Dissolution diagram

The PVA/CA, PVA/CA/β-CD, and PVA/CA/γ-CD dissolution diagram is showing in Fig. 9. The dissolved concentration of CA increased with slowly increasing time. In the case of PVA/CA nanofibers dissolving much slower compared to the PVA/CA/β-CD and PVA/CA/γ-CD nanofibers due to inclusion complex formation between the CA and CDs. The PVA/CA/γ-CD dissolved slightly faster than PVA/CA/β-CD nanofiber's initial concentration was reached at 14.8 mM and increased concerning time (min). Finally, this result

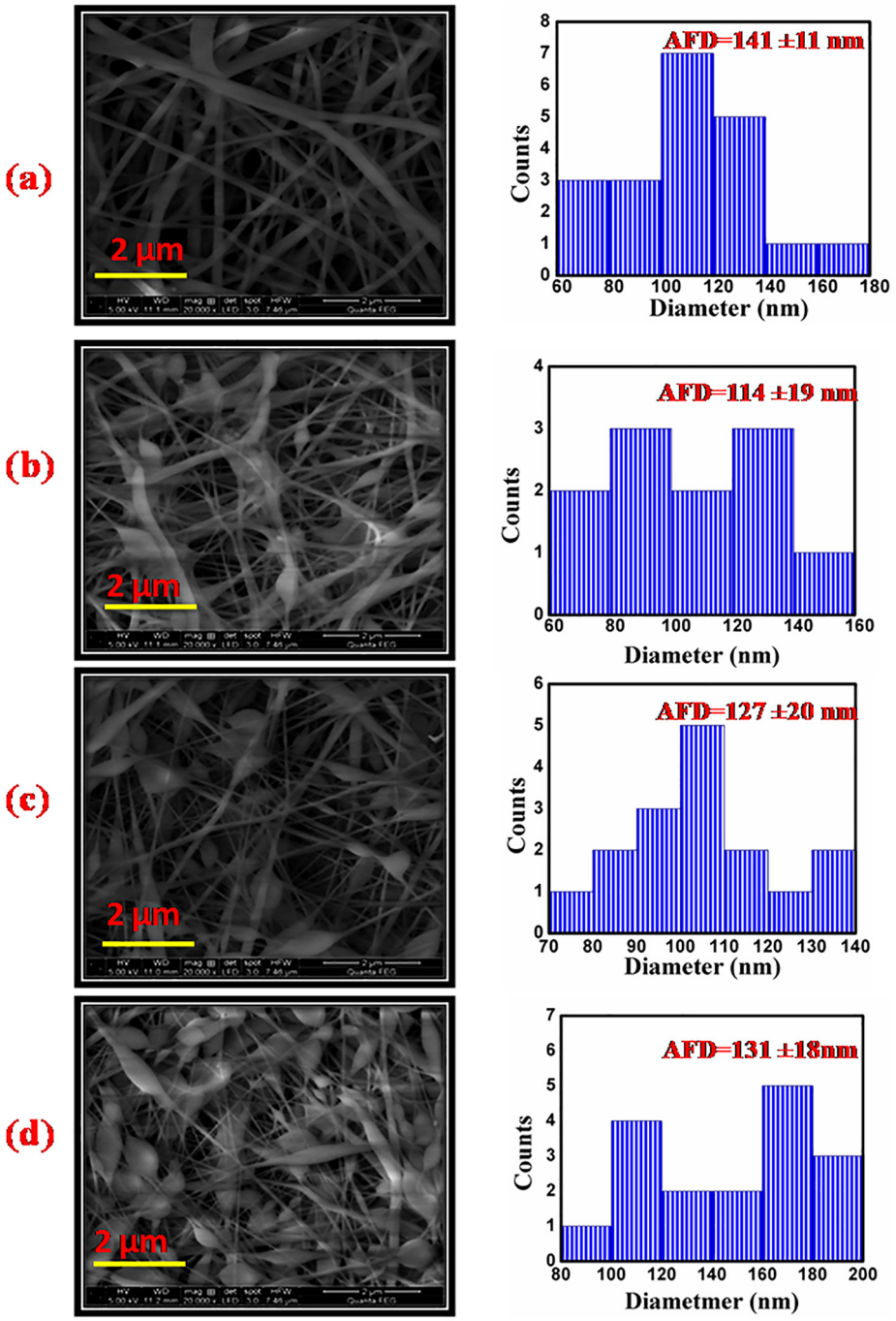

Fig. 7. SEM image and Average Fiber Diameter (AFD) of prepared nanofibers (a) PVA, (b) VA/CA, (c) PVA/CA/β-CD, and (d) PVA/CA/γ-CD.

indicates that the presence of CDs in the nanofibers is influencing to enhance the CA dissolving from the nanofibers.

3.8. In vitro anti-bacterial activity

The PVA/CA/β-CD and PVA/CA/γ-CD nanofibers antibacterial activity are have tested against gram-positive and other bacteria.

In Fig. 10 the antibacterial activity of both nanofibers' inhibition in the growth of both bacteria due to the CA is the well-known antibacterial agent. Fig. 10b PVA/CA/γ-CD nanofibers were wider than PVA/CA/β-CD nanofibers; because CA includes with γ-CD cavity binding constant was much higher so, enhanced the CA solubility in agar medium. The enhanced antibacterial activity of CA/γ-CD embedding PVA electrospun nanofibers can be achieving the excellent physical properties of CA with a large surface area to volume ratio of nanofibers. Thus, the above result clearly explained that CDs/CA embedded electrospun nanofibers have to develop the active antibacterial material that may be applicable in the food industry.

4. Conclusion

Here, first, we prepared the solid CA/CDs using β-CD and γ-CD by a simple co-precipitation method. The FT-IR result mentions the chemical interaction between the CA and CDs to the formation of the inclusion complex. Besides, UV, ^{1}H NMR, and Raman-spectroscopy indicate that CA presents and interacts with the CD cavity in the CA/CD. Additionally, the phase solubility results

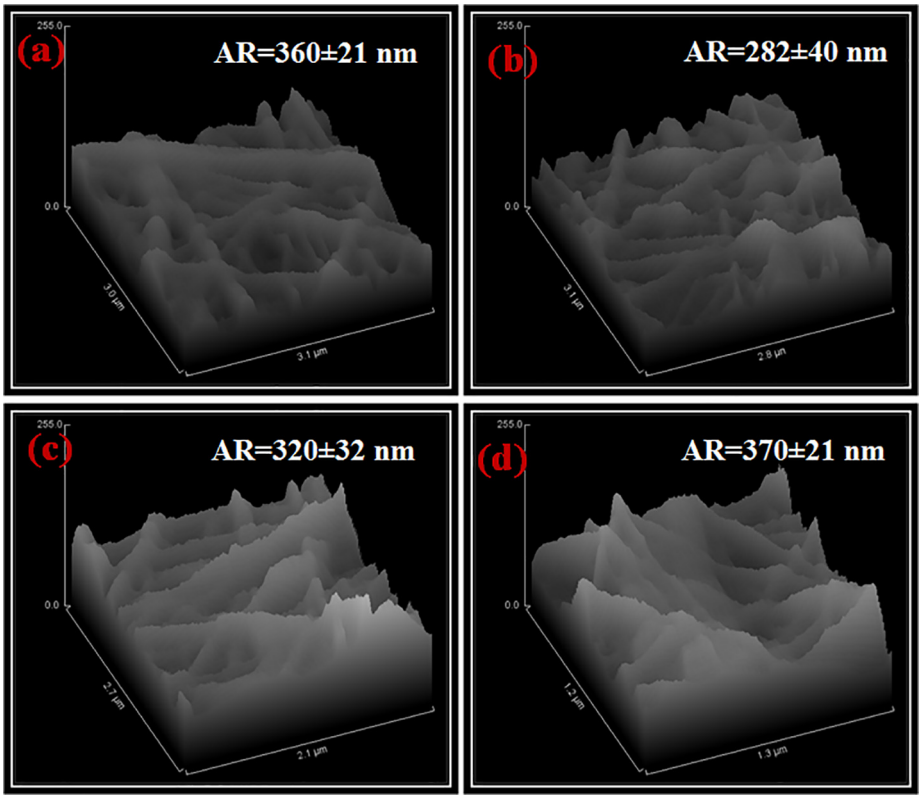

Fig. 8. Average Roughness (AR) of the prepared nanofibers (a) PVA, (b) PVA/CA, (c) PVA/CA/β-CD, and (d) PVA/CA/γ-CD.

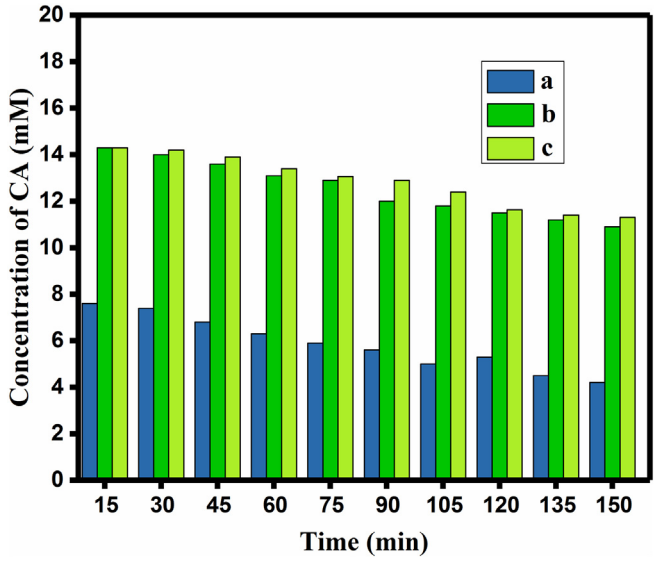

Fig. 9. Dissolution diagram of CA from (a) PVA/CA, (b) PVA/CA/β-CD, and (c) PVA/CA/γ-CD nanofibers.

revealed that the solubility of CA increased linearly with increasing the CDs concentration. The electrospinning technique is have used to fabricate the CA/CDs. It is incorporating into PVA electrospun nanofibers. To our result that smooth and uniform bead nanofibers are have obtained by SEM images. Besides, dissolution studies are have obtained by using absorbance data of UV-Spectrum at 283 nm; the dissolution diagram of CA in PVA/CA/CDs is much slower than PVA/CA electrospun nanofibers due to ICs between CA and CDs. More importantly, the case of PVA/CA/CDs is showing better antibacterial activity results against *S. aureus* and *E. coli* due to enhanced solubility of CA and in PVA/CA/CDs nanofibers in agar medium. CA is a bio-active compound as well as an antibacterial agent so, which is widely using in the food industry. Finally, our result suggests that CA/CDs are embedding into PVA electrospun nanofibers having high surface area, high porosity, and antibacterial activity so, which material may be in the food industry and food preservative, etc.

CRediT authorship contribution statement

Vimalasruthi Narayanan: Conceptualization. **Manawwer Alam:** . **Naushad Ahmad:** Validation. **Suganya Bharathi Balakrishnan:** Methodology. **Vigneshkumar Ganesan:** Investigation. **Esakkimuthu Shanmugasundaram:** Resources. **Brindha Rajagopal:** Investigation. **Stalin Thambusamy:** Supervision.

Declaration of Competing Interest

The authors declare that they have no known competing financial interests or personal relationships that could have appeared to influence the work reported in this paper.

Acknowledgment

Manawwer Alam is grateful to the Research Supporting Project number (RSP-2020/113), Saud University, Riyadh, Saudi Arabia for support. **Vimalasruthi Narayanan** gratefully acknowledges the Department of Science and Technology (DST) India, under the scheme of the DST-INSPIRE Programme [No. IF 180377] to carry out this work, and **Dr. Stalin Thambusamy** likes to thank RUSA-Phase 2.0 grant No. F. 24-51/2014-U, Policy (TNMulti-Gen), Dept. of Edn., Govt. of India, Dt.09.10.2018.

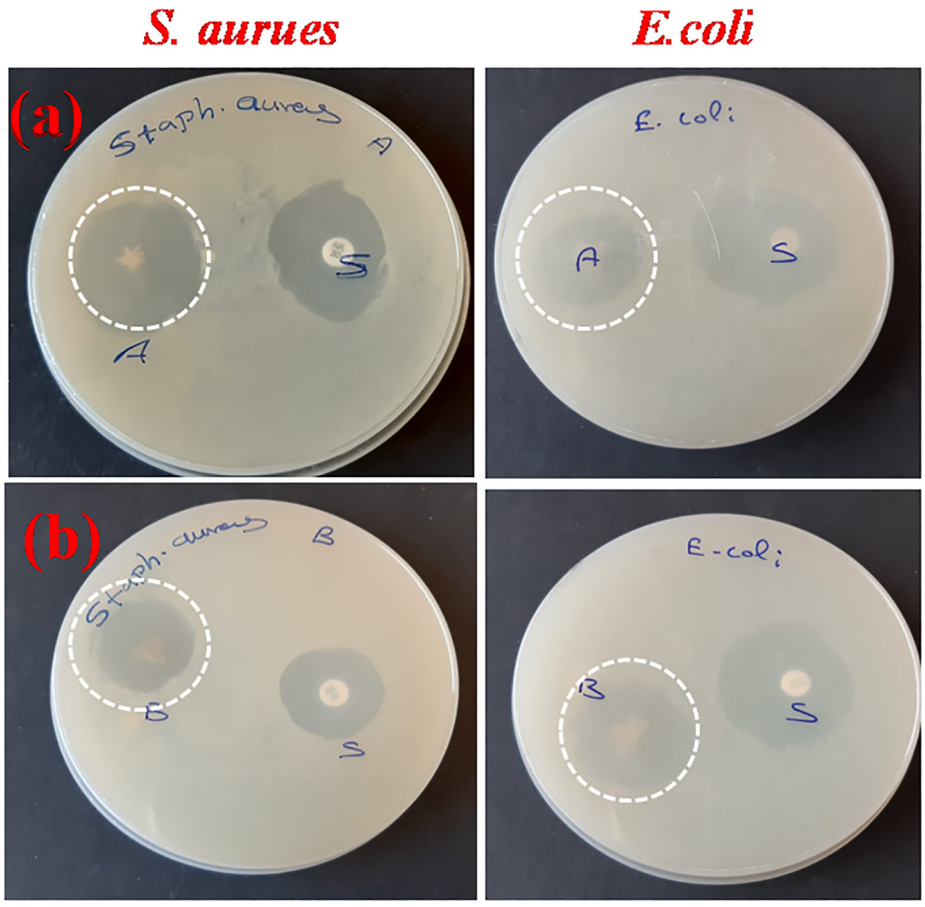

Fig. 10. Antibacterial activity of (a) PVA/ CA/β-CD and (b) PVA/CA/ γ-CD nanofibers.

References

[1] T.T. More, J.S.S. Yadav, S. Yan, R.D. Tyagi, R.Y. Surampalli, Extracellular polymeric substances of bacteria and their potential environmental applications, J. Environ. Manage. 144 (2014) 1–25.

[2] F. Zia, K.M. Zia, M. Zuber, S. Kamal, N. Aslam, Starch based polyurethanes: A critical review updating recent literature, Carbohydr. Polym. 134 (2015) 784–798.

[3] G.R. Guillen, Y. Pan, M. Li, E.M.V. Hoek, Preparation and characterization of membranes formed by nonsolvent induced phase separation: A review, Ind. Eng. Chem. Res. 50 (2011) 3798–3814.

[4] M.M. Munir, H. Widiyandari, F. Iskandar, K. Okuyama, Patterned indium tin oxide nanofiber films and their electrical and optical performance, Nanotechnology. 19 (2008) 375601.

[5] H. Sehaqui, N. Ezekiel Mushi, S. Morimune, M. Salajkova, T. Nishino, L.A. Berglund, Cellulose nanofiber orientation in nanopaper and nanocomposites by cold drawing, ACS Appl. Mater. Interfaces. 4 (2012) 1043–1049.

[6] I. Stassen, M. Styles, G. Grenci, H. Van Gorp, W. Vanderlinden, S. De Feyter, P. Falcaro, D. De Vos, P. Vereecken, R. Ameloot, Chemical vapour deposition of zeolitic imidazolate framework thin films, Nat. Mater. 15 (2016) 304–310.

[7] K.A. Khalil, H. Fouad, T. Elsarnagawy, F.N. Almajhdi, Preparation and characterization of electrospun PLGA/silver composite nanofibers for biomedical applications, Int. J. Electrochem. Sci. 8 (2013) 3483–3493.

[8] S. Zhang, Fabrication of novel biomaterials through molecular self-assembly, Nat. Biotechnol. 21 (2003) 1171–1178.

[9] T. Subbiah, G.S. Bhat, R.W. Tock, S. Parameswaran, S.S. Ramkumar, Electrospinning of nanofibers, J. Appl. Polym. Sci. 96 (2005) 557–569.

[10] N. Bhardwaj, S.C. Kundu, Electrospinning: A fascinating fiber fabrication technique, Biotechnol. Adv. 28 (2010) 325–347.

[11] J. Xue, W.u. Tong, Y. Dai, Y. Xia, Electrospinning and Electrospun Nanofibers: Methods, Materials, and Applications, Chem Rev. 119 (8) (2019) 5298–5415.

[12] A. Formhals, et al. Method and apparatus for spinning, U.S. Patent 2,349,950, Issue date: May 30, 1944.

[13] A. Asti, L. Gioglio, Natural and synthetic biodegradable polymers: Different scaffolds for cell expansion and tissue formation, Int. J. Artif. Organs. 37 (3) (2014) 184–205.

[14] L.J. Villarreal-Gómez, J.M. Cornejo-Bravo, R. Vera-Graziano, D. Grande, Electrospinning as a powerful technique for biomedical applications: A critically selected survey, J. Biomater. Sci. Polym. Ed. 27 (2) (2016) 157–176.

[15] F. Mokhtari, M. Salehi, F. Zamani, F. Hajiani, F. Zeighami, M. Latifi, Advances in electrospinning: The production and application of nanofibres and nanofibrous structures, Text. Prog. 119–219 (2016).

[16] B. Suganya Bharathi, T. Stalin, Preparation of silver nanoparticles and riboflavin embedded electrospun polymer nanofibrous scaffolds for in vivo wound dressing application, Process Biochem. 88 (2020) 148–158.

[17] B. Suganya Bharathi, T. Stalin, Cerium oxide and peppermint oil loaded polyethylene oxide/graphene oxide electrospun nanofibrous mats as antibacterial wound dressings, Mater. Today Commun. 21 (2019) 10664.

[18] K. Škrlec, Š. Zupančič, S. Prpar Mihevc, P. Kocbek, J. Kristl, A. Berlec, Development of electrospun nanofibers that enable high loading and long-term viability of probiotics, Eur. J. Pharm. Biopharm. 136 (2019) 108–119.

[19] Y. Zhou, D. Yang, X. Chen, Q. Xu, F. Lu, J. Nie, Electrospun water-soluble carboxyethyl chitosan/poly(vinyl alcohol) nanofibrous membrane as potential wound dressing for skin regeneration, Biomacromolecules. 9 (2008) 349–354.

[20] C. Zhang, L. Wang, T. Zhai, X. Wang, Y. Dan, L.S. Turng, The surface grafting of graphene oxide with poly(ethylene glycol) as a reinforcement for poly(lactic acid) nanocomposite scaffolds for potential tissue engineering applications, J. Mech. Behav. Biomed. Mater. 53 (2016) 403–413.

[21] W. Nuansing, S. Ninmuang, W. Jarernboon, S. Maensiri, S. Seraphin, Structural characterization and morphology of electrospun TiO2 nanofibers, Mater. Sci. Eng. B Solid-State Mater. Adv. Technol. 131 (2006) 144–155.

[22] D. Li, M.W. Frey, A.J. Baeumner, Electrospun polylactic acid nanofiber membranes as substrates for biosensor assemblies, J. Memb. Sci. 279 (2006) 354–363.

[23] F. Ajalloueian, H. Tavanai, J. Hilborn, O. Donzel-Gargand, K. Leifer, A. Wickham, A. Arpanaei, Emulsion electrospinning as an approach to Fabricate PLGA/chitosan nanofibers for biomedical applications, Biomed Res. Int. (2014), Article Id 475280.

[24] Y.Z. Zhang, J. Venugopal, Z.M. Huang, C.T. Lim, S. Ramakrishna, Characterization of the surface biocompatibility of the electrospun PCL-Collagen nanofibers using fibroblasts, Biomacromolecules. 6 (2005) 2583–2589.

[25] C. Yuan, Z. Jin, X. Xu, H. Zhuang, W. Shen, Preparation and stability of the inclusion complex of astaxanthin with hydroxypropyl-β-cyclodextrin, Food Chem. 109 (2008) 264–268.

[26] A. Celebioglu, Z.I. Yildiz, T. Uyar, Thymol/cyclodextrin inclusion complex nanofibrous webs: Enhanced water solubility, high thermal stability and antioxidant property of thymol, Food Res. Int. 106 (2018) 280–290.

[27] M. Kfoury, D. Landy, S. Ruellan, L. Auezova, H. Greige-Gerges, S. Fourmentin, Nootkatone encapsulation by cyclodextrins: Effect on water solubility and photostability, Food Chem. 136 (2017) 41–48.
[28] Z.I. Yildiz, A. Celebioglu, M.E. Kilic, E. Durgun, T. Uyar, Menthol/cyclodextrin inclusion complex nanofibers: Enhanced water-solubility and high-temperature stability of menthol, J. Food Eng. 224 (2018) 27–36.
[29] B. Göttel, J.M. de Souza e Silva, C. Santos de Oliveira, F. Syrowatka, M. Fiorentzis, A. Viestenz, A. Viestenz, K. Mäder, Electrospun nanofibers – A promising solid in-situ gelling alternative for ocular drug delivery, Eur. J. Pharm. Biopharm. 146 (2020) 125–132.
[30] Ivan M Savic, Vesna D. Nikolic, Ivana M. Savic Gajic, Ljubisa B. Nikolic, Blaga C. Radovanović, Jelena Mladenović, Investigation of properties and structural characterization of the quercetin inclusion complex with (2-hydroxypropyl)-β-cyclodextrin, J. Incl. Phenom. Macro. 82 (2015) 383–394.
[31] Ivana Lj, Ivan M. Nikolic, Mirjana M. Savic, Srdjan J. Popsavin, Tatjana M. Rakic, Mihajilov- Krstev, Ivan S. Ristic, Suzana P. Eric, Ivana M. Savic-Gajic, Preparation, characterization and antimicrobial activity of inclusion complex of biochanin A with (2-hydroxypropyl)- β-cyclodextrin, J. Pharm. Pharmacol. 70 (2018) 1485–1493.
[32] I. Savic-Gajic, I.M. Savic, V.D. Nikolic, L.B. Nikolic, M.M. Popsavin, A.J. Kapor, Study of the solubility, photostability and structure of inclusion complexes of carvedilol with β- cyclodextrin and (2-hydroxypropyl)- β-cyclodextrin, J. Incl. Phenom. Macrocycl. Chem. 86 (2016) 7–17.
[33] I.M. Savic, J. Emilija, V.D. Nikolic, M.M. Popsavin, S.J. Rakic, I.M. Savic-Gajic, The effect of com plexation with cyclodextrins on the antioxidant and antimicrobial activity of ellagic acid, Pharm. Dev. Technol. 24 (2018) 1–27.
[34] V.J. Stella, Q. He, Cyclodextrins, Toxicol. Pathol. 36 (1) (2008) 30–42.
[35] S.V. Kurkov, T. Loftsson, Cyclodextrins, Int. J. Pharm. 453 (1) (2013) 167–180.
[36] A. Shanmuga Priya, B. Suganya Bharathi, Giribabu Veerakanellore, T. Stalin, In-vitro dissolution rate and molecular docking studies of cabergoline drug with β-cyclodextrin, J. Mol. Struct. 1160 (2018) 1–8.
[37] S.P. Arumugam, S.B. Balakrishnan, V. Ganesan, M. Munisamy, S.V. Kuppu, V. Narayanan, V. Baskaralingam, S. Jeyachandran, S. Thambusamy, In-vitro dissolution and microbial inhibition studies on anticancer drug etoposide with β-cyclodextrin, Mater. Sci. Eng. C. 102 (2019) 96–105.
[38] S.R.S. Rudrangi, W. Kaialy, M.U. Ghori, V. Trivedi, M.J. Snowden, B.D. Alexander, Solid-state flurbiprofen and methyl-β-cyclodextrin inclusion complexes prepared using a single-step, organic solvent-free supercritical fluid process, Eur. J. Pharm. Biopharm. 104 (2016) 164–170.
[39] T. Loftsson, M.E. Brewster, Pharmaceutical applications of cyclodextrins. 1. Drug solubilization and stabilization, J. Pharm. Sci. 85 (10) (1996) 1017–1025.
[40] R. Challa, A. Ahuja, J. Ali, R.K. Khar, Cyclodextrins in drug delivery: An updated review, AAPS PharmSciTech. 6 (2) (2005) E329–E357.
[41] N. Sharma, A. Baldi, Exploring versatile applications of cyclodextrins: An overview, Drug Deliv. 23 (3) (2016) 739–757.
[42] P. Berben, J. Stappaerts, M.J.A. Vink, E. Domínguez-Vega, G.W. Somsen, J. Brouwers, P. Augustijns, Linking the concentrations of itraconazole and 2-hydroxypropyl-β-cyclodextrin in human intestinal fluids after oral intake of Sporanox®, Eur. J. Pharm. Biopharm. 132 (2018) 231–236.
[43] M.P. Abuçafy, B.L. Caetano, B.G. Chiari-Andréo, B. Fonseca-Santos, A.M. do Santos, M. Chorilli, L.A. Chiavacci, Supramolecular cyclodextrin-based metal-organic frameworks as efficient carrier for anti-inflammatory drugs, Eur. J. Pharm. Biopharm. 127 (2018) 112–119.
[44] T. Uyar, Y. Nur, J. Hacaloglu, F. Besenbacher, Electrospinning of functional poly (methyl methacrylate) nanofibers containing cyclodextrin-menthol inclusion complexes, Nanotechnology. 20 (12) (2009) 125703.
[45] F. Kayaci, Y. Ertas, T. Uyar, Enhanced thermal stability of eugenol by cyclodextrin inclusion complex encapsulated in electrospun polymeric nanofibers, J. Agric. Food Chem. 61 (34) (2013) 8156–8165.
[46] F. Kayaci, T. Uyar, Encapsulation of vanillin/cyclodextrin inclusion complex in electrospun polyvinyl alcohol (PVA) nanowebs: Prolonged shelf-life and high temperature stability of vanillin, Food Chem. 61 (34) (2012) 8156–8165.
[47] A. Celebioglu, F. Kayaci-Senirmak, S. Ipek, E. Durgun, T. Uyar, Polymer-free nanofibers from vanillin/cyclodextrin inclusion complexes: High thermal stability, enhanced solubility and antioxidant property, Food Funct. 7 (7) (2016) 3141–3153.
[48] K.A. Rieger, J.D. Schiffman, Electrospinning an essential oil: Cinnamaldehyde enhances the antimicrobial efficacy of chitosan/poly(ethylene oxide) nanofibers, Carbohydr. Polym. 113 (2014) 561–568.
[49] Z. Aytac, S.I. Kusku, E. Durgun, T. Uyar, Encapsulation of gallic acid/cyclodextrin inclusion complex in electrospun polylactic acid nanofibers: Release behavior and antioxidant activity of gallic acid, Mater. Sci. Eng. C. 63 (2016) 231–239.
[50] A.P.F. Monteiro, C.M.S.L. Rocha, M.F. Oliveira, S.M.L. Gontijo, R.R. Agudelo, R.D. Sinisterra, M.E. Cortés, Nanofibers containing tetracycline/β-cyclodextrin: Physico-chemical characterization and antimicrobial evaluation, Carbohydr. Polym. 156 (2017) 417–426.
[51] M. Zamani, M. Morshed, J. Varshosaz, M. Jannesari, Controlled release of metronidazole benzoate from poly ε-caprolactone electrospun nanofibers for periodontal diseases, Eur. J. Pharm. Biopharm. 75 (2) (2010) 179–185.
[52] F. Perret, M. Duffour, Y. Chevalier, H. Parrot-Lopez, Design, synthesis, and in vitro evaluation of new amphiphilic cyclodextrin-based nanoparticles for the incorporation and controlled release of acyclovir, Eur. J. Pharm. Biopharm. 83 (2013) 25–32.
[53] T. Suchý, M. Šupová, E. Klapková, V. Adamková, J. Závora, M. Žaloudková, Š. Rýglová, R. Ballay, F. Denk, M. Pokorný, P. Sauerová, M. Hubálek Kalbáčová, L. Horný, J. Veselý, T. Voňavková, R. Průša, The release kinetics, antimicrobial activity and cytocompatibility of differently prepared collagen/hydroxyapatite/vancomycin layers: Microstructure vs. nanostructure, Eur. J. Pharm. Sci. 100 (2017) 219–229.
[54] T. Suchý, M. Šupová, P. Sauerová, M. Hubálek Kalbáčová, E. Klapková, M. Pokorný, L. Horný, J. Závora, R. Ballay, F. Denk, M. Sojka, L. Vištejnová, Evaluation of collagen/hydroxyapatite electrospun layers loaded with vancomycin, gentamicin and their combination: Comparison of release kinetics, antimicrobial activity and cytocompatibility, Eur. J. Pharm. Biopharm. 140 (2019) 50–59.
[55] I. Gülçin, Antioxidant activity of caffeic acid (3,4-dihydroxycinnamic acid), Toxicology. (2006). [52] M.R. Olthof, P.C.H. Hollman, M.B. Katan, Human Nutrition and Metabolism Chlorogenic Acid and Caffeic Acid Are Absorbed in Humans 1, J. Nutr. 217 (2001) 213–220.
[56] M. Zhang, J. Li, L. Zhang, J. Chao, Preparation and spectral investigation of inclusion complex of caffeic acid with hydroxypropyl-β-cyclodextrin, Spectrochim. Acta - Part A Mol. Biomol, Spectrosc. 71 (2009) 1891–1895.
[57] K. Ramasamy, S. Thambusamy, Dual emission and pH based naphthalimide derivative fluorescent sensor for the detection of Bi3+, Sensors Actuators, B Chem. 247 (2017) 632–640.
[58] T. Stalin, P. Vasantha Rani, B. Shanthi, A. Sekar, N. Rajendiran, Inclusion complex of 1, 2, 3-trihydroxy benzene with α-and β-cyclodextrins, Indian J. Chem. Sec A 45 (2006) 1113–1120.
[59] S. Mohandoss, T. Stalin, Photochemical and computational studies of inclusion complexes between β-cyclodextrin and 1,2-dihydroxyanthraquinones, Photochem. Photobiol. Sci. 16 (4) (2017) 476–488.
[60] K. Srinivasan, S. Radhakrishnan, T. Stalin, Inclusion complexes of β-cyclodextrin-dinitrocompounds as UV absorber for ballpoint pen ink, Spectrochim. Acta - Part A Mol. Biomol. Spectrosc. 129 (2014) 551–564.
[61] K. Srinivasan, T. Stalin, Studies on inclusion complexes of 2,4-dinitrophenol, 2,4-dinitroaniline, 2,6-dinitroaniline and 2,4-dinitrobenzoic acid incorporated with β-cyclodextrin used for a novel UV absorber for ballpoint pen ink, J. Incl. Phenom. Macrocycl. Chem. 78 (1–4) (2014) 337–350.
[62] K. Sivakumar, M. Parameswari, T. Stalin, Etodolac:β-cyclodextrin inclusion complex as a novel fluorescent chemosensor probe for Ba2+, J. Carbohydr. Chem. 35 (2) (2016) 118–130.
[63] N.H.A. Ngadiman, M.Y. Noordin, D. Kurniawan, A. Idris, A.S.A. Shakir, Influence of Polyvinyl Alcohol Molecular Weight on the Electrospun Nanofiber Mechanical Properties, Procedia Manuf. 2 (2015) 568–572.
[64] N. Georgieva, R. Bryaskova, R. Tzoneva, New Polyvinyl alcohol-based hybrid materials for biomedical application, Mater. Lett. 88 (2012) 19–22.
[65] T. Higuchi, K.A. Connors, Phase Solubility Techniques, Adv. Anal. Chem. Instrum. (1965).
[66] S.W. Jun, M.S. Kim, J.S. Kim, H.J. Park, S. Lee, J.S. Woo, S.J. Hwang, Preparation and characterization of simvastatin/hydroxypropyl-β-cyclodextrin inclusion complex using supercritical antisolvent (SAS) process, Eur. J. Pharm. Biopharm. 66 (3) (2007) 413–421.
[67] D. Arrua, M.C. Strumia, M.A. Nazareno, Immobilization of caffeic acid on a polypropylene film: Synthesis and antioxidant properties, J. Agric. Food Chem. 58 (2010) 9228–9234.
[68] P.R.K. Mohan, G. Sreelakshmi, C.V. Muraleedharan, R. Joseph, Water soluble complexes of curcumin with cyclodextrins: Characterization by FT-Raman spectroscopy, Vib. Spectrosc. 62 (2012) 77–84.
[69] A.M. Da Silva, Food antioxidants cyclodextrin inclusion compounds: Molecular spectroscopic studies and molecular modelling, Macrocycl. Chem. New Res. Dev. (2010).
[70] C.S. Mangolim, C. Moriwaki, A.C. Nogueira, F. Sato, M.L. Baesso, A.M. Neto, G. Matioli, Curcumin-β-cyclodextrin inclusion complex: Stability, solubility, characterisation by FT-IR, FT-Raman, X-ray diffraction and photoacoustic spectroscopy, and food application, Food Chem. 153 (2014) 361–370.
[71] V.T. Karathanos, I. Mourtzinos, K. Yannakopoulou, N.K. Andrikopoulos, Study of the solubility, antioxidant activity and structure of inclusion complex of vanillin with β-cyclodextrin, Food Chem. 101 (2007) 652–658.
[72] N.A. Hotaling, K. Bharti, H. Kriel, C.G. Simon, DiameterJ: A validated open source nanofiber diameter measurement tool, Biomaterials. 61 (2015) 327–338.
[73] F. Kayaci, O.C.O. Umu, T. Tekinay, T. Uyar, Antibacterial electrospun poly(lactic acid) (PLA) nanofibrous webs incorporating triclosan/cyclodextrin inclusion complexes, J. Agric. Food Chem. 61 (16) (2013) 3901–3908.